

Cholesteryl Oligoarginine Delivering Vascular Endothelial Growth Factor siRNA Effectively Inhibits Tumor Growth in Colon Adenocarcinoma

Won Jong Kim,¹ Lane V. Christensen,¹ Seongbong Jo,¹ James W. Yockman,¹ Ji Hoon Jeong,¹ Yong-Hee Kim,² and Sung Wan Kim^{1,*}

¹Center for Controlled Chemical Delivery, Department of Pharmaceutics and Pharmaceutical Chemistry, 20 S 2030 E RM 205 BPRB, University of Utah, Salt Lake City, UT 84112-5820, USA

²Department of Bioengineering, College of Engineering, Hanyang University, Seoul 133-791, Korea

*To whom correspondence and reprint requests should be addressed. Fax: +1 801 581 7848. E-mail: rburns@pharm.utah.edu.

Available online 12 June 2006

Vascular endothelial growth factor (VEGF) is a multifunctional angiogenic growth factor that is a primary stimulant of the development and maintenance of a vascular network in the vascularization of solid tumors. It has been reported that a blockade of VEGF-mediated angiogenesis is a powerful method for tumor regression. RNA interference represents a naturally occurring biological strategy for inhibition of gene expression. In mammalian systems, however, the *in vivo* application of small interfering RNA (siRNA) is severely limited by the instability and poor bioavailability of unmodified siRNA molecules. In this study, we tested the hypothesis that a hydrophobically modified protein transduction domain, cholesteryl oligo-D-arginine (Chol-R9), may stabilize and enhance tumor regression efficacy of the VEGF-targeting siRNA. The noncovalent complexation of a synthetic siRNA with Chol-R9 efficiently delivered siRNA into cells *in vitro*. Moreover, in a mouse model bearing a subcutaneous tumor, the local administration of complexed VEGF-targeting siRNA, but not of scrambled siRNA, led to the regression of the tumor. Hence, we propose a novel and simple system for the local *in vivo* application of siRNA through Chol-R9 for cancer therapy.

Key Words: VEGF, angiogenesis, RNA interference, oligoarginine, gene therapy

INTRODUCTION

The phenomenon of RNA interference (RNAi) or posttranscriptional gene silencing is an evolutionarily conserved biological response to double-stranded RNA (dsRNA) for degradation of the sequence-specific homologous mRNA. RNAi is initiated by the dsRNA-specific endonuclease, Dicer, which promotes processive cleavage of long dsRNA into double-stranded fragments between 21 and 23 nucleotides long, termed small interfering RNA (siRNA). This siRNA binds to the RNA-induced silencing complex, which recognizes target mRNA to be degraded [1–4]. Recently, it has become a useful tool for specific gene silencing and analysis of gene function.

To improve the efficiency of siRNA function, delivery systems need to be developed to condense siRNA effectively into small particles, thereby enhancing the cellular uptake and protection from enzymatic degradation. Ideas for siRNA delivery vehicles based upon the designs of polymeric delivery systems for plasmid DNA [5–9] have begun to flourish [10,11]; therefore, enhancement of the

transfection efficiency *in vitro* and *in vivo* has progressed rapidly. In fact, numerous attempts to enhance siRNA function have been made based on cationic lipopeptide [12], steroid and lipid conjugates of siRNA [13,14], and block copolymer-coated calcium phosphate nanoparticles [15]. Recently, to enhance the cellular uptake and transfection efficiency, arginine-rich cell-penetrating peptides (CPPs) such as human immunodeficiency virus (HIV-1) TAT and antennapedia have been developed as gene delivery vehicles [16,17]. In cell culture, a conjugate of an antisense oligonucleotide and the antennapedia peptide was able to inhibit the translation of amyloid precursor protein at a concentration of 40 nM [18]. In a separate study, the antennapedia peptide-conjugated oligonucleotide against Cu/Zn superoxide dismutase showed a 100-fold higher efficiency in culture than did the oligonucleotide itself [19]. Furthermore, arginine oligopeptides have been modified with several hydrophobic lipid molecules to enhance plasmid gene transfection [20]. The mechanism of internalization of CPPs is

not well understood and has recently been the subject of discussion. Most cellular uptake studies of CPPs in the literature based on fluorescence microscopy of fixed cells and/or flow cytometry analysis report that internalization of CPPs does not involve endocytosis [21–25]. These studies have been recently revisited by the mechanism of cellular uptake being reevaluated. More current evidence shows that the internalization of CPPs is an energy-dependent process involving classical adsorptive endocytosis [26–28].

We have reported an effective water-soluble lipopolymer (WSLP) by combining the cationic headgroup of branched polyethylenimine (bPEI; M_w 1.8 kDa) with a hydrophobic lipid anchor, cholesterol chloroformate [6]. WSLP showed low cytotoxicity and enhanced transfection efficacy *in vitro* and *in vivo* [6,29–31]. The effectiveness of WSLP over bPEI was due to the modification of the inherent structural DNA complex to enhance the interaction with plasma membrane and facilitate the endosomal escape.

In this study, we synthesized a cholesteryl oligo-D-arginine (nine residues) conjugate (Chol-R9) as a siRNA delivery vehicle for vascular endothelial growth factor (VEGF) silencing. VEGF is a growth factor most consistently found in a wide variety of conditions associated

with angiogenesis [32]. It has been reported that impairing the function of VEGF could inhibit tumor growth and metastasis by preventing its own vascularization in a variety of animal models [33–35]. We investigated the potency of the Chol-R9 conjugate as a siRNA delivery vehicle *in vitro* and *in vivo* in a mouse tumor model.

RESULTS

Synthesis of Chol-R9

We successfully modified oligoarginine (R9) with cholesteryl chloroformate (Fig. 1). The ^1H NMR spectrum of Chol-R9 showed characteristic cholesteryl methyl proton peaks ranging from 0.5 to 1.0 ppm (Fig. 2A). R9 proton peaks are also shown in the spectrum. Especially the methine proton peak of R9 (protons at α -carbons), which represents nine protons, appeared at 4.2 ppm. We determined the coupling yield of cholesteryl chloroformate to R9 from the cholesteryl methyl proton peak at 0.5 ppm, which represents three protons, and the proton peak of arginine α -carbon at 4.2 ppm using the equation

$$\text{coupling yield (\%)} = (3 \times A_{0.5\text{ppm}}) / A_{4.2\text{ppm}} \times 100,$$

where $A_{0.5\text{ ppm}}$ and $A_{4.2\text{ ppm}}$ stand for integrations of proton peaks at 0.5 and 4.2 ppm in the NMR spectrum of

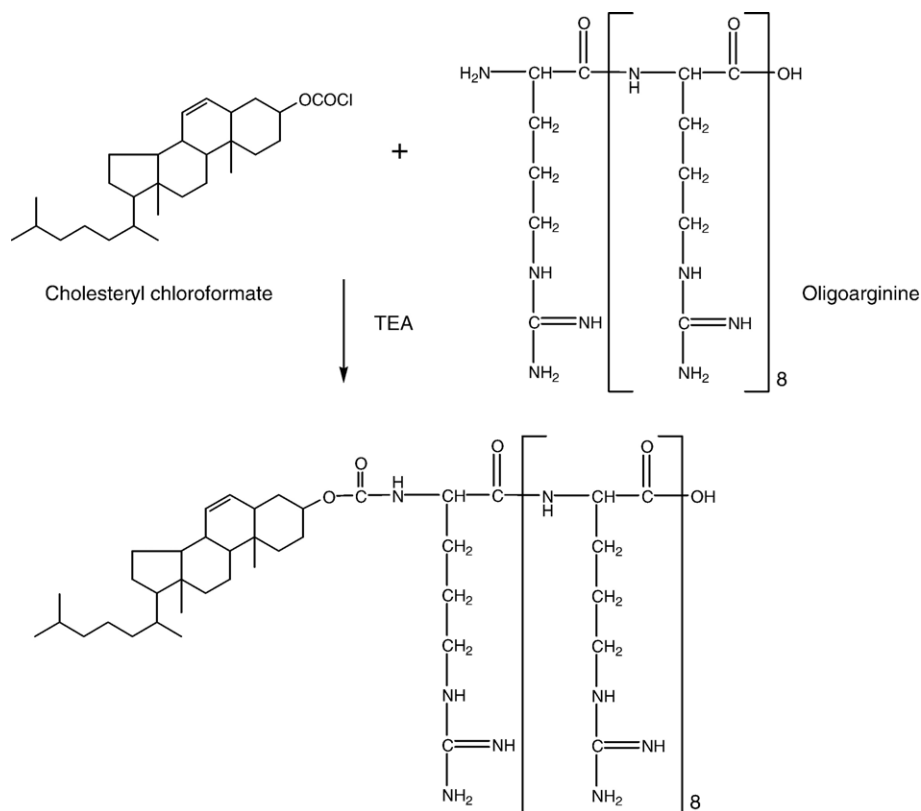


FIG. 1. Synthesis scheme of Chol-R9 conjugate.

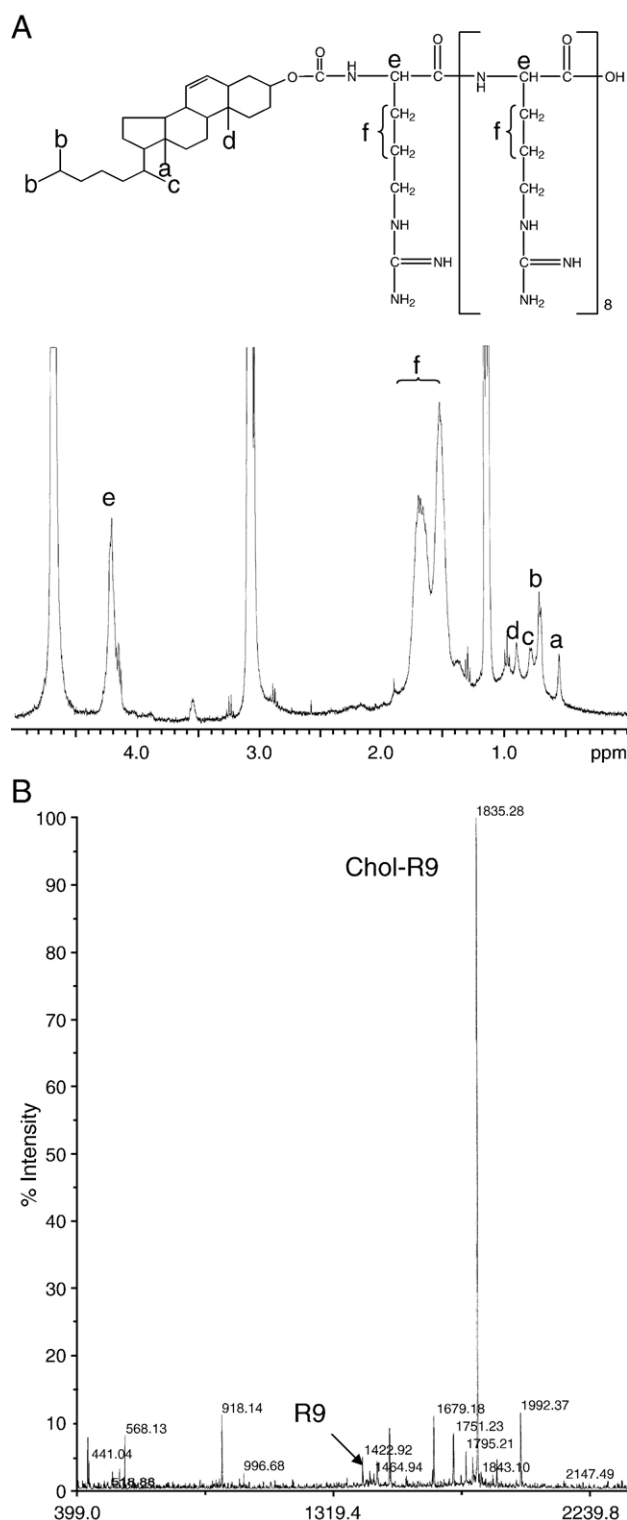


FIG. 2. Chol-R9 conjugate characterized using ^1H NMR and MALDI-TOF mass spectroscopy. (A) ^1H NMR spectrum of Chol-R9. (B) MALDI-TOF mass spectra of Chol-R9.

Chol-R9, respectively. The calculated coupling yield in this study was 50.3%. The matrix-assisted laser desorption time-of-flight (MALDI-TOF) mass spectrum of Chol-R9 showed a predominant peak at 1835.28 (m/z), which can be assigned as (M-H) (Fig. 2B). The electrospray ionization (ESI) mass spectrum also showed dominant peaks of Chol-R9 and R9, indicating an absence of any free cholesterol chloroformate (data not shown). These results reaffirm the fact that the polymer product contains only a mixture of Chol-R9 and R9.

Complex Formation of Chol-R9 with Plasmid DNA

To identify the characteristics of Chol-R9 to act as an efficient nonviral gene carrier, we carried out DNA complex formation on agarose gel electrophoresis at different N/P ratios, i.e., the ratio of concentration of total nitrogen atoms (N) of the polycation to that of the phosphate groups (P) of reporter plasmid DNA. The movement of plasmid in the gel was retarded as the amount of the Chol-R9 conjugate was increased, demonstrating that the conjugate binds to negatively charged DNA, neutralizing its charge (Fig. 3A, top). Complete complex formations were achieved at N/P ratios equal to and above 8:1 (lane 5), similar to unmodified oligoarginine (Fig. 3A, bottom).

Cell Toxicity and *in Vitro* Transfection Efficiency of Chol-R9/DNA Complex

We investigated the cytotoxicity of Chol-R9/DNA complexes using the 3-(4,5-dimethylthiazol-2-yl)-2,5-diphenyltetrazolium bromide (MTT) assay (Fig. 3B) on 293T cells. We prepared Chol-R9/DNA complexes at various N/P ratios from 8 to 72, while we made bPEI/DNA complexes at an N/P ratio of 5. The complex of Chol-R9/DNA showed at least 90% cell viability at the N/P ratios of 8 to 48.

We evaluated the transfection efficiency of the synthesized Chol-R9 *in vitro* using 293T cell lines. For the transfection experiments, we formulated various Chol-R9/pCMV-Luc or R9/pCMV-Luc complexes with a fixed amount of pCMV-Luc (50 $\mu\text{g}/\text{ml}$). Chol-R9/pCMV-Luc complexes showed higher transfection efficiency than R9/pCMV-Luc complexes at a range of N/P ratios between 20 and 40 (Fig. 3C). The conjugation of cholesterol to R9 suggests enhanced cellular uptake of complexes and increased transfection efficiency.

Complex Formation of Chol-R9 Conjugate with siRNA

To identify the formation of Chol-R9/siRNA complexes, we performed polyacrylamide gel electrophoresis (PAGE) at different N/P ratios. The positively charged R9 of the Chol-R9 conjugate makes complexes with the negatively charged phosphate ions on the base backbone on siRNA. When the value of the N/P ratio of Chol-R9/siRNA reached 40, free siRNA was not detected on the PAGE (Fig. 4B).

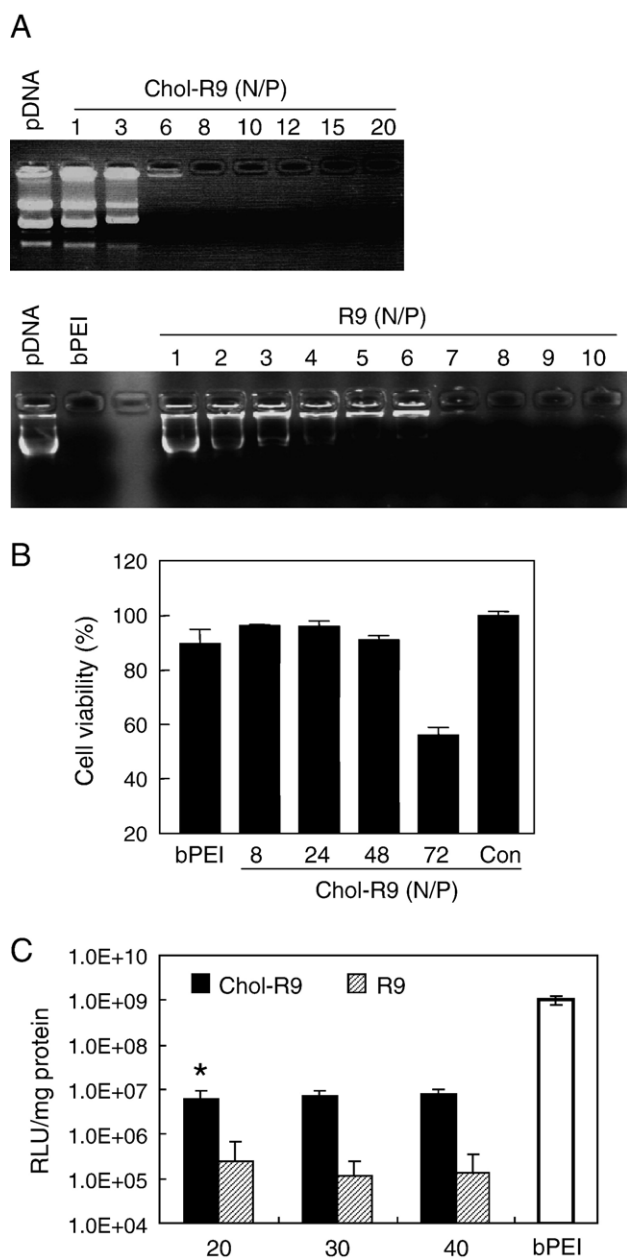


FIG. 3. Complex formation, cell viability, and transfection profiles of Chol-R9/plasmid DNA. (A) Electrophoretic patterns of plasmid DNA complexes with Chol-R9 (top) and R9 (bottom). (B) Cytotoxicity of bPEI/pCMV-Luc and Chol-R9/pCMV-Luc for 293T cells. The data are expressed as mean values \pm standard deviation of three experiments. (C) Luciferase expression of Chol-R9 conjugates compared to unmodified R9 and a bPEI control. The graph represents mean values \pm standard deviation of experiments run in triplicate. * $P < 0.05$ compared to unmodified R9.

VEGF Silencing Effect of Chol-R9/siRNA Complex *in Vitro*

To evaluate the biological significance of these systems, we investigated the inhibitory activity of siRNA against the expression of VEGF in CT-26 cells. We evaluated the

inhibitory effect from the relative silencing of the VEGF assayed by enzyme-linked immunosorbent assay (ELISA). Obviously, we observed appreciable silencing of the VEGF for the bPEI/siVEGF complex at the N/P ratio of 10, while scrambled (sc) VEGF showed no effect (Fig. 5A). As shown in Fig. 5B, Chol-R9/siVEGF complex suppressed the VEGF production by 55% compared with the untreated control, whereas the unmodified R9/siVEGF complex did not silence the expression of VEGF with the same amount of siRNA.

Inhibition of Tumor Growth with Chol-R9/siRNA Complex *in Vivo*

We injected CT-26 cells (1×10^6) sc into the flank of mice. By 2 weeks, visible tumors had developed at the injection sites (mean tumor volume 74.18 mm³). To determine the therapeutic effectiveness of VEGF siRNA, we started intratumoral treatment with Chol-R9/siVEGF or Chol-R9/scVEGF and repeated every 4 days for a total of six times. As shown in Figs. 6A and 6B, Chol-R9/siVEGF complex markedly suppressed the tumor growth compared with Chol-R9/scVEGF complex ($P < 0.05$) or 5% glucose solution as a control. To assess the relationship between the therapeutic effects of Chol-R9/siRNA and VEGF in tumors, we quantified the amount of VEGF in tumors. We observed a dramatically lower level of VEGF in tumors treated with Chol-R9/siVEGF at 17 days after the first injection, whereas the tumors treated with Chol-R9/scVEGF showed higher level of VEGF (Fig. 7A). We then examined the vascularization in tumors by immunostaining with an anti-CD31 antibody. The vascularization in tumors observed in the Chol-R9/siVEGF-treated group was significantly reduced compared with tumors from the Chol-R9/scVEGF-treated group (Fig. 7B). Based on the above observations, we believe that the antitumor effect of Chol-R9/siVEGF was due mainly to the antiangiogenic effect of Chol-R9/siVEGF, which was confirmed by VEGF quantification (Fig. 7A) and histological examination (Fig. 7B).

DISCUSSION

Since siRNAs play a pivotal role in gene silencing, the critical factors that will determine the success of RNA interference approaches are the ability to deliver intact siRNAs efficiently into the appropriate cells. In an attempt to enhance the function of siRNA, numerous studies have used DNA vectors that, upon viral or nonviral transfection, lead to intracellular expression of double-stranded RNA [36–40]. While this approach often results in robust downregulation of gene expression *in vitro*, it suffers *in vivo* from problems including low transfection efficiency, poor tissue penetration, and toxicity to the host.

Bioactive arginine-rich peptides derived from HIV-1 TAT and antennapedia homeodomain capable of con-

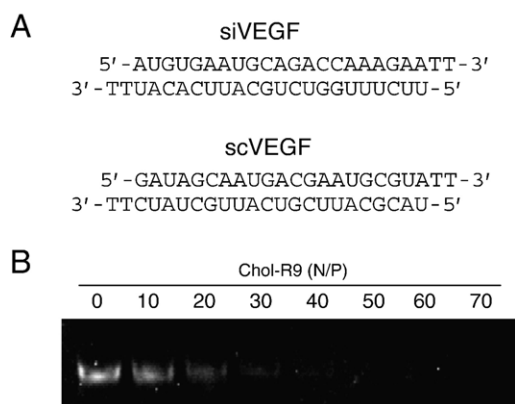


FIG. 4. Sequences of siRNA and complex formation profile. (A) Sequences of siRNA targeting VEGF, siVEGF, and scrambled siRNA, scVEGF. (B) Electrophoretic patterns of siRNA complexes with Chol-R9 conjugates.

densing nucleic acids have attracted considerable attention as parts of DNA and siRNA delivery vectors because of a highly reproducible and scalable production and an inherent specific biological activity [16–20]. Cellular uptake of these peptides has been ascribed in the literature to an energy- and receptor-independent mechanism that does not involve endocytosis [21–25]. Recently, however, it has been demonstrated that cell fixation, even under mild conditions, leads to the artifactual uptake of these peptides [26]. Moreover, a number of studies questioned the validity of the predominant mechanisms and suggested that the internalization of arginine-rich peptides is a temperature- and energy-dependent process involving endocytosis [26–28]. When used alone, small arginine-rich peptides usually exhibit lower cytotoxicity and are also weaker activators of the complement system than high-molecular-weight polycations such as bPEI. However, the polyelectrolyte complexes formed with short arginine-rich peptides lack sufficient stability to survive in the blood circulation and showed lower cellular uptake.

Small peptides of a distinctive structure, such as oligoarginine, have been studied less extensively compared with other cationic polymers as a DNA or siRNA delivery vehicle. Wender *et al.* reported that short oligomers of arginine were indeed more efficiently taken up into cells than TAT peptide [41]. This was quantified further by Michaelis–Menten kinetics analysis that showed that the arginine oligomers (R9) had K_m values 20- and 100-fold greater than that found for TAT. Prompted by this potential value of oligoarginine to enhance cellular entry, we initiated modification of oligoarginine to improve its transfection ability further.

Previously, the conjugation of the hydrophobic lipid anchor cholesterol to cationic polymers of polyethylenimine was reported to enhance the cellular uptake of DNA from the cell surface [6,7,29–31,42]. This WSLP con-

denses DNA and enhances endosomal release due to its tertiary amines, while the lipid coating on the DNA increases its permeability through cell membranes. To magnify advantages of the cell-penetrating oligoarginine and cholesterol lipid, we conjugated the cholesterol lipid anchor to R9 covalently as a gene and siRNA delivery vehicle.

For gene transfer, bPEI of high-molecular-weight (M_w 25 kDa) is commonly used, but is highly toxic to the cells even at low N/P ratios. Addition of the cholesterol to R9 did not adversely affect cell viability even at higher N/P ratios, though it increased transfection efficiency significantly in 293T cells (Figs. 3B and 3C). This higher

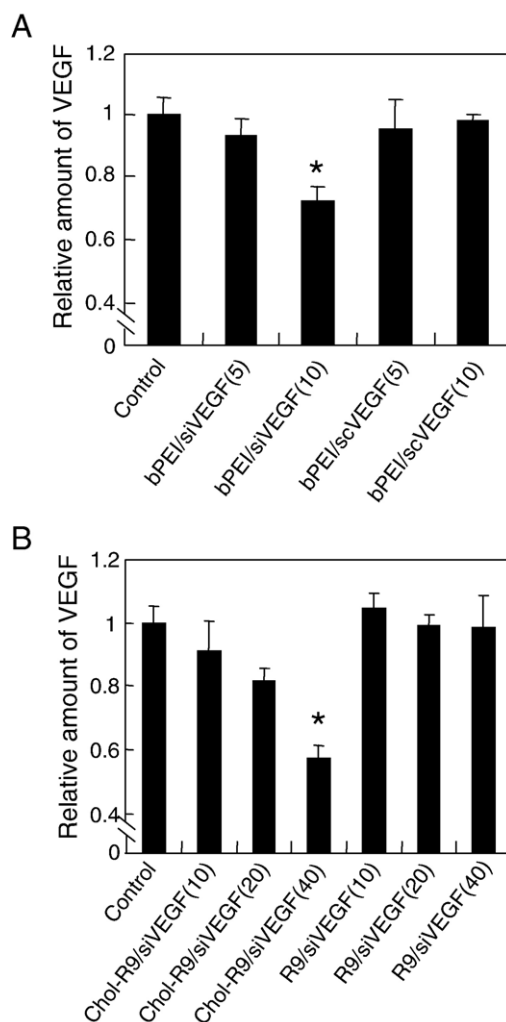


FIG. 5. VEGF silencing with a complex of siRNAs (siVEGF, VEGF siRNA; scVEGF, VEGF scrambled siRNA) and various carriers in CT-26 cells. (A) Sequence specificity of siRNAs. Cells were transfected with bPEI/siVEGF and bPEI/scVEGF at the N/P ratios of 5 and 10. (B) Comparison of Chol-R9 with unmodified R9. Cells were transfected with Chol-R9/siVEGF and R9/siVEGF at the N/P ratios of 10 to 40. VEGF concentration in the conditioned medium was determined by ELISA for mouse VEGF. * $P < 0.02$ compared to untreated control.

transfection efficiency suggests enhanced cellular uptake of complexes.

To test for the bioactivity of Chol-R9 complexed with siRNAs, we performed a study of the inhibition of tumor angiogenesis by siRNA. A number of growth factors have been identified as potential positive regulators of angiogenesis. Among them, VEGF has been thoroughly studied as a target for antiangiogenic therapy [8,33–35]. Recently, inhibition of VEGF production by siRNA was reported as an effective and useful method for tumor antiangiogenic therapy *in vitro* and *in vivo* [43–45].

In this study, we show that the combination of two independent agents (oligoarginine and cholesterol) can produce synergistic effects and not only inhibit the production of VEGF in CT-26 cells *in vitro* but also suppress tumor growth *in vivo*. The higher bioactivity of Chol-R9/siRNA might be due to the ionic and hydrophobic interactions between Chol-R9 and siRNA, while the precise mechanism is not still clear. In a recent report,

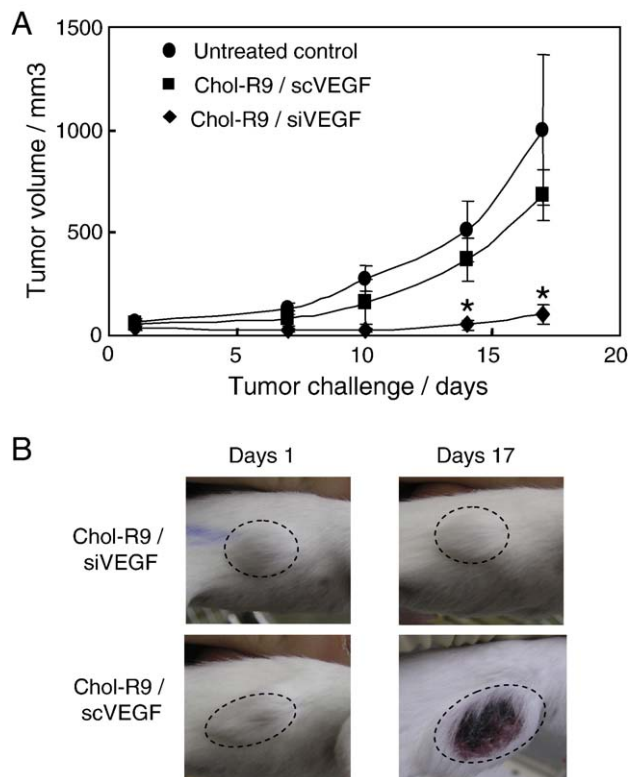


FIG. 6. Antitumor effect of siRNAs *in vivo*. (A) Tumor growth curves. VEGF siRNA (10 μ M siVEGF) or VEGF scrambled siRNA (10 μ M scVEGF) was mixed with Chol-R9 conjugate at the N/P ratio of 40, and 50 μ l of each mixture was injected into the tumor region subcutaneously. As a control, 5% glucose solutions were injected. Day 1 corresponds to 2 weeks after inoculation of cells when the tumor volume was approximately 70 mm³. Tumor diameters were measured at a regular intervals for up to 17 days with calipers, and the tumor volume was calculated. Results represent the means \pm standard deviation ($n = 5$ tumors). * $P < 0.05$ compared to Chol-R9/scVEGF. (B) Images of CT-26 allografts. On days 1 and 17 CT-26 tumors were taken.

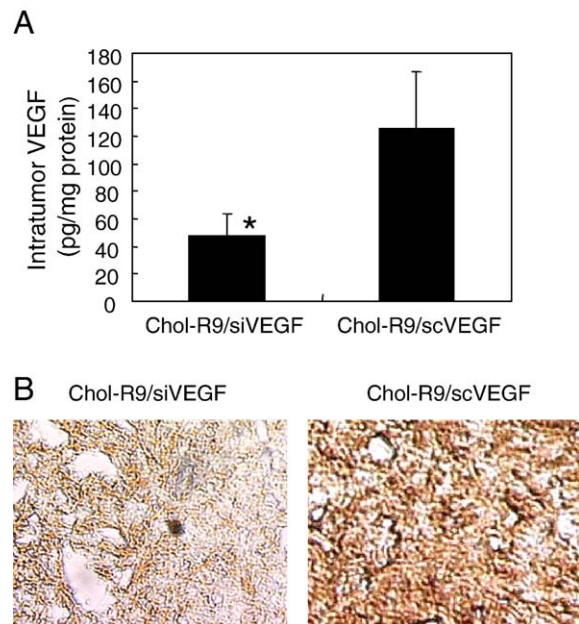


FIG. 7. Intratumoral VEGF contents and vascularization. (A) VEGF levels in tumors at 17 days after injection. The excised tumors were homogenized in PBS with protease inhibitor (Sigma Chemical Co.) and then centrifuged. The amount of VEGF in each supernatant was measured by ELISA. * $P < 0.05$ compared to Chol-R9/scVEGF. (B) Immunohistochemical staining of the subcutaneous tumors with CD31 antibody. Representative images of Chol-R9/siVEGF-treated tumors (left) and Chol-R9/scVEGF-treated tumors (right).

higher cellular association of the stearyl-R8/DNA than R8/DNA was observed by Khalil *et al.* [46]. They suggested that with the aid of both the cationic charges and the hydrophobic interactions the stearyl-R8/DNA complexes would be adsorbed at high levels to the cell surface and then internalized via endocytosis. Conjugation of hydrophobic moieties to peptides has also been described to enhance the transfection efficiency by causing the compaction of DNA/carrier complexes [6,7,29–31,47,48].

Taken together, we suggest that the combination of the cholesterol moiety and cationic cell-penetrating peptides may enhance the cellular uptake of Chol-R9/siRNA complexes and transfection efficiency via endocytosis. Further study is needed to investigate the precise internalizing mechanisms of Chol-R9 or Chol-R9/siRNA complexes, including the intracellular location and fate of Chol-R9/siRNA complexes. Moreover, a variety of lipid moieties might be conjugated to arginine-rich peptides to test their enhancing ability for siRNA delivery.

MATERIALS AND METHODS

Synthesis of cholesteryl oligoarginine conjugate. Chol-R9 was synthesized by reacting cholesterol chloroformate (Aldrich Chemical Co.) and oligo-D-arginine (nine residues) (Genemed Synthesis, Inc., San Francisco, CA, USA) in the presence of triethylamine (TEA) (Fig. 1). Oligoarginine (15.4 mg, 10.8 μ mol) was dissolved in 5 ml of anhydrous dimethylformamide.

After 15.08 μ l of TEA was added into the oligoarginine solution, cholesterol chloroformate (24.3 mg, 54 μ mol) in 5 ml of anhydrous tetrahydrofuran was slowly added at room temperature. The reaction mixture was stirred overnight. Upon completion of the reaction, solvents were removed by purging dry nitrogen gas through a glass transfer pipette. The remaining cholesterol chloroformate and TEA were rinsed off three times with 15 ml of diethyl ether each time. The crude precipitate was purified for 2 days by dialysis (MWCO 500; Spectrum) against deionized distilled water to remove free cholesterol. Fourteen milligrams of Chol-R9 was finally collected after freeze drying. Synthesized Chol-R9 was characterized by ^1H NMR spectroscopy, MALDI-TOF, and ESI mass spectrophotometer.

Gel retardation assay. Chol-R9/plasmid DNA complex formation were confirmed by the agarose gel retardation assay. Chol-R9/pCMV-luc complexes were formed at different N/P ratios by incubating in 5% glucose solution at room temperature for 30 min. Each sample was then analyzed by electrophoresis on a 1% agarose gel with ethidium bromide (EtBr; 0.1 μ g/ml). Complex formation of Chol-R9/siRNA was monitored by the polyacrylamide gel retardation assay. siRNA targeting mouse VEGF (siVEGF) and scrambled siRNA (scVEGF) were purchased from IDT Technologies, Inc. (Coralville, IA, USA). Sequences of siRNA are shown in Fig. 4A. We selected siRNA sequences as reported by Filleur *et al.* [45]. Various amounts of Chol-R9, ranging from 0 to 44.5 ng, were added to 7 ng of siRNA at Chol-R9/siRNA N/P ratios from 0 to 70 in 5% glucose solution and incubated for 30 min at room temperature. After incubation, each sample was electrophoresed on 13% polyacrylamide gel (w/v) for 1 h at 100 V. TBE (89 mM Tris-borate, 2 mM EDTA) buffer was used as electrophoresis buffer. Following EtBr (0.1 μ g/ml) staining, the gel was illuminated with a UV illuminator to show the location of the siRNA.

Cell toxicity and in vitro transfection assay. The cytotoxicity of Chol-R9/DNA complexes was investigated using a tetrazolium-based calorimetric assay as previously reported [49]. In this test, viability of cells is assessed by the metabolism of a water-soluble tetrazolium dye, MTT, into insoluble formazan salts (Sigma) (Fig. 3B). Briefly, 293T cells were plated in 24-well plates at 60,000 cells per well and allowed to incubate for 24 h. Polymer/DNA complexes were added in triplicate to the wells at 0.5 μ g reporter plasmid DNA per well at varying N/P ratios. The bPEI (M_r 25 kDa) control was prepared at a 5:1 N/P ratio. After 44 h of incubation, the cell viability was determined, in which viability was compared to cells that received 5% glucose instead of polyplex dispersion.

Luciferase expression using different N/P ratios of R9 and Chol-R9 was observed by using a pCMV-Luc reporter plasmid. When cells reached ~80% confluency, transfections were performed at the total DNA concentration of 50 μ g/ml. Transfection experiments were carried out on 293T cells in six-well plates maintained in DMEM (GIBCO) medium at 37°C in a humidified atmosphere containing 5% CO₂. After 4 h of incubation, medium was replaced with 2 ml of fresh medium supplemented with 10% fetal bovine serum (FBS; Hyclone) and the cells were cultured for 48 h. Luciferase expression was quantified using the Luciferase Assay System (Promega) normalized by milligrams of protein.

ELISA. CT-26 colon adenocarcinoma cells were grown to 80% confluency in 24-well plates and transfected with cationic substance/siRNA complexes. Following 24-h incubation, the level of mouse VEGF produced in the medium was determined by using a mouse VEGF ELISA kit (R&D Systems, Inc., Minneapolis, MN, USA) according to the recommendation of the manufacturer's protocol. Briefly, the 96-microwell plate (provided in the kit), coated with mouse polyclonal anti-VEGF antibody, was washed with wash buffer. Cell supernatant samples were diluted 1:4 by calibrator diluent, and 50 μ l of the sample was added into the designated wells. Similarly, VEGF standards ranging from 7.8 to 500 pg/ml, also diluted in calibrator diluent, were added to the microwell plates. The calibrator diluent alone was added in a blank well and incubated at room temperature for 2 h. After being washed four times with wash buffer, 100 μ l of polyclonal antibody against VEGF conjugated to horseradish peroxidase was added and incubated at room temperature for 2 h. After the wells were washed again four times, tetramethylbenzidine substrate

solution was added and incubated at room temperature for 30 min. The enzymatic reaction was stopped by adding 100 μ l of stop solution to the wells, and absorbance was determined by spectrophotometric reading at 450 nm. The VEGF concentration in the cell supernatant samples was calculated based on the standard curve.

Cell culture. 293T and CT-26 colon adenocarcinoma cell lines were grown and maintained in DMEM and RPMI 1640, respectively, which were supplemented with 10% FBS at 37°C and humidified 5% CO₂.

VEGF silencing with Chol-R9/siRNA complex in vitro. CT-26 cells were seeded in 24-well tissue culture plates at 8×10^4 cells per well in 10% FBS containing RPMI 1640 medium. Cells achieved 80% confluency within 24 h after which they were transfected with cationic substance/siRNA complexes prepared at different N/P ratios ranging from 5 to 40. The total amount of siRNA loaded was maintained constant at 0.7 μ g/well. The transfection was carried out in the absence of serum. The cells were allowed to incubate at 37°C in the presence of complexes for 4 h in a CO₂ incubator followed by replacement of 1 ml of RPMI 1640 containing 10% FBS. Thereafter, the cells were incubated at 37°C for additional 24 h. Cell supernatants were collected for analysis of the amount of VEGF produced by ELISA.

Tumor therapy. To generate tumors, 4- to 5-week-old female BALB/c mice were injected subcutaneously in the middle of the right flank with 100 μ l of a single-cell suspension containing 1×10^6 CT-26 cells. Tumor size was measured using a vernier caliper across its longest (a) and shortest (b) diameters and its volume was calculated using the formula $V = 0.5ab^2$. Treatment of the tumors was started after 10–15 days when the tumor size reached approximately 70 mm³. Chol-R9/siRNA complexes (N/P ratio of 40) were prepared in 5% glucose and 50 μ l of the complexes was injected directly into the tumor of BALB/c mice at a dose of 3.5 μ g siRNA/mouse. The tumors were measured every 4 days and mice were examined for appearance and growth of necrosis as well as decreased physical activity. Tumor progression was reported in terms of tumor volume over a period of 2 weeks.

Statistical analysis. Results are reported as means \pm SD. The statistical analysis between groups was determined using a nonpaired *t* test. $P < 0.05$ was considered significant.

ACKNOWLEDGMENT

This work was supported by National Institutes of Health Grant CA10707.

RECEIVED FOR PUBLICATION NOVEMBER 10, 2004; REVISED MARCH 14, 2006; ACCEPTED MARCH 20, 2006.

REFERENCES

- Zamore, P. D., Tuschl, T., Sharp, P. A., and Bartel, D. P. (2000). RNAi: double-stranded RNA directs the ATP-dependent cleavage of mRNA at 21 to 23 nucleotide intervals. *Cell* **101**: 25–33.
- Elbashir, S. M., Lendeckel, W., and Tuschl, T. (2001). RNA interference is mediated by 21- and 22-nucleotide RNAs. *Genes Dev.* **15**: 188–200.
- Opalinska, J. B., and Gewirtz, A. M. (2002). Nucleic-acid therapeutics: basic principles and recent applications. *Nat. Rev. Drug Discovery* **1**: 503–514.
- Elbashir, S. M., Harborth, J., Lendeckel, W., Yalcin, A., Weber, K., and Tuschl, T. (2001). Duplexes of 21-nucleotide RNAs mediate RNA interference in cultured mammalian cells. *Nature* **411**: 494–498.
- Kim, J. -S., Maruyama, A., Akaike, T., and Kim, S. W. (1997). In vitro gene expression on smooth muscle cells using a terplex delivery system. *J. Controlled Release* **47**: 51–59.
- Han, S., Mahato, R. I., and Kim, S. W. (2001). Water-soluble lipopolymer for gene delivery. *Bioconjugate Chem.* **12**: 337–345.
- Furgeson, D. Y., Chan, W. S., Yockman, J. W., and Kim, S. W. (2003). Modified linear polyethylenimine-cholesterol conjugates for DNA complexation. *Bioconjugate Chem.* **14**: 840–847.
- Kim, W. J., *et al.* (2005). Soluble Flt-1 gene delivery using PEI-g-PEG-RGD conjugate for anti-angiogenesis. *J. Controlled Release* **106**: 224–234.
- Jeong, J. H., *et al.* (2005). Anti-GAD antibody targeted non-viral gene delivery to islet beta cells. *J. Controlled Release* **107**: 562–570.
- Bologna, J. C., Dorn, G., Natt, F., and Weiler, J. (2003). Linear polyethylenimine as a

- tool for comparative studies of antisense and short double-stranded RNA oligonucleotides. *Nucleosides Nucleotides Nucleic Acids* **23**: 1729–1731.
11. Urban-Klein, B., Werth, S., Abuharheid, S., Czubyko, F., and Aigner, A. (2005). RNAi-mediated gene-targeting through systemic application of polyethylenimine (PEI)-complexed siRNA in vivo. *Gene Ther.* **12**: 461–466.
 12. Unnamalai, N., Kang, B. G., and Lee, W. S. (2004). Cationic oligopeptide-mediated delivery of dsRNA for post-transcriptional gene silencing in plant cells. *FEBS J.* **566**: 307–310.
 13. Lorenz, C., Hadwiger, P., John, M., Vormlocher, H.-P., and Unverzagt, C. (2004). Steroid and lipid conjugates of siRNAs to enhance cellular uptake and gene silencing in liver cells. *Bioorg. Med. Chem. Lett.* **14**: 4975–4977.
 14. Spagnou, S., Miller, A. D., and Keller, M. (2004). Lipidic carriers of siRNA: differences in the formulation, cellular uptake, and delivery with plasmid DNA. *Biochemistry* **43**: 13348–13356.
 15. Kakizawa, Y., Furukawa, S., and Kataoka, K. (2004). Block copolymer-coated calcium phosphate nanoparticles sensing intracellular environment for oligodeoxynucleotide and siRNA delivery. *J. Controlled Release* **97**: 345–356.
 16. Rudolph, C., et al. (2003). Oligomers of the arginine-rich motif of the HIV-1 TAT protein are capable of transferring plasmid DNA into cells. *J. Biol. Chem.* **278**: 11411–11418.
 17. Manickam, D. S., Bisht, H. S., Wan, L., Mao, G., and Oupicky, D. (2005). Influence of TAT-peptide polymerization on properties and transfection activity of TAT/DNA polyplexes. *J. Controlled Release* **102**: 293–306.
 18. Allinquant, B., Hantraye, P., Mailloux, P., Moya, K., Bouillot, C., and Prochiantz, A. (1995). Downregulation of amyloid precursor protein inhibits neurite outgrowth in vitro. *J. Cell Biol.* **128**: 919–927.
 19. Troy, C. M., Derossi, D., Prochiantz, A., Greene, L. A., and Shelanski, M. L. (1996). Downregulation of Cu/Zn superoxide dismutase leads to cell death via the nitric oxide-peroxynitrite pathway. *J. Neurosci.* **16**: 253–261.
 20. Futaki, S., et al. (2001). Stearylarginine-rich peptides: a new class of transfection systems. *Bioconjugate Chem.* **12**: 1005–1011.
 21. Suzuki, T., Futaki, S., Niwa, M., Tanaka, S., Ueda, K., and Sugiura, Y. (2002). Possible existence of common internalization mechanisms among arginine-rich peptides. *J. Biol. Chem.* **277**: 2437–2443.
 22. Torchilin, V. P., Rammohan, R., Weissig, V., and Levechenko, T. S. (2001). Tat peptide on the surface of liposomes affords their efficient intracellular delivery even at low temperature and in presence of metabolic inhibitors. *Proc. Natl. Acad. Sci. USA* **98**: 8786–8791.
 23. Futaki, S., et al. (2001). Arginine-rich peptides: an abundant source of membrane-permeable peptides having potential as carriers for intracellular protein delivery. *J. Biol. Chem.* **276**: 5836–5840.
 24. Vives, E., Brodin, P., and Lebleu, B. (1997). A truncated HIV-1 Tat protein basic domain rapidly translocates through the plasma membrane and accumulates in the cell nucleus. *J. Biol. Chem.* **272**: 16010–16017.
 25. Derossi, D., Chassing, G., and Prochiantz, A. (1998). Trojan peptides: the penetration system for intracellular delivery. *Trends Cell Biol.* **8**: 84–87.
 26. Richard, J. P., et al. (2003). Cell-penetrating peptides: a reevaluation of the mechanism of cellular uptake. *J. Biol. Chem.* **278**: 585–590.
 27. Lecifert, J. A., Harkins, S., and Whitton, J. L. (2002). Full-length proteins attached to the HIV tat protein transduction domain are neither transduced between cells, nor exhibit enhanced immunogenicity. *Gene Ther.* **9**: 1422–1428.
 28. Drin, G., Cottin, S., Blanc, E., Rees, A. R., and Temsamani, J. (2003). Studies on the internalization mechanism of cationic cell-penetrating peptides. *J. Biol. Chem.* **278**: 31192–31201.
 29. Yockman, J. W., Maheshwari, A., Han, S., and Kim, S. W. (2003). Tumor regression by repeated intratumoral delivery of water soluble lipopolymers/p2CMVml-12 complexes. *J. Controlled Release* **87**: 177–186.
 30. Lee, M., Rentz, J., Han, S., Bull, D. A., and Kim, S. W. (2003). Water-soluble lipopolymer as an efficient carrier for gene delivery to myocardium. *Gene Ther.* **10**: 585–593.
 31. Lee, M., Rentz, J., Bikram, M., Han, S., Bull, D. A., and Kim, S. W. (2003). Hypoxia-inducible VEGF gene delivery to ischemic myocardium using water-soluble lipopolymer. *Gene Ther.* **10**: 1535–1542.
 32. Leung, D. W., Cachianes, G., Kuang, W. J., Goeddel, D. V., and Ferrara, N. (1989). Vascular endothelial growth factor is a secreted angiogenic mitogen. *Science* **246**: 1306–1309.
 33. Kim, K. J., et al. (1993). Inhibition of vascular endothelial growth factor-induced angiogenesis suppresses tumour growth in vivo. *Nature* **362**: 841–844.
 34. Brekken, R. A., et al. (2000). Selective inhibition of vascular endothelial growth factor (VEGF) receptor 2 (KDR/Flk-1) activity by a monoclonal anti-VEGF antibody blocks tumor growth in mice. *Cancer Res.* **60**: 5117–5124.
 35. Holash, J., et al. (2002). VEGF-Trap: a VEGF blocker with potent antitumor effects. *Proc. Natl. Acad. Sci. USA* **99**: 11393–11398.
 36. Xia, H., Mao, Q., Paulson, H. L., and Davidson, B. L. (2002). siRNA-mediated gene silencing in vitro and in vivo. *Nat. Biotechnol.* **20**: 1006–1010.
 37. McCaffrey, A. P. (2003). Inhibition of hepatitis B virus in mice by RNA interference. *Nat. Biotechnol.* **21**: 639–644.
 38. Jacque, J.-M., Triques, K., and Stevenson, M. (2002). Modulation of HIV-1 replication by RNA interference. *Nature* **418**: 435–438.
 39. Coburn, G. A., and Cullen, B. R. (2002). Potent and specific inhibition of human immunodeficiency virus type 1 replication by RNA interference. *J. Virol.* **76**: 9225–9231.
 40. Kapadia, S. B., Brideau-Andersen, A., and Chisari, F. V. (2003). Interference of hepatitis C virus RNA replication by short interfering RNAs. *Proc. Natl. Acad. Sci. USA* **100**: 2014–2018.
 41. Wender, P. A., et al. (2000). The design, synthesis, and evaluation of molecules that enable or enhance cellular uptake: peptidic molecular transporters. *Proc. Natl. Acad. Sci. USA* **97**: 13003–13008.
 42. Kurisawa, M., Yokoyama, M., and Okano, T. (2000). Transfection efficiency increases by incorporating hydrophobic monomer units into polymeric gene carriers. *J. Controlled Release* **68**: 1–8.
 43. Lu, P. Y., Xie, F. Y., and Woodle, M. C. (2003). siRNA-mediated antitumorogenesis for drug target validation and therapeutics. *Curr. Opin. Mol. Ther.* **5**: 225–234.
 44. Takei, Y., Kadomatsu, K., Yuzawa, Y., Matsuo, S., and Muramatsu, T. (2004). A small interfering RNA targeting vascular endothelial growth factor as cancer therapeutics. *Cancer Res.* **64**: 3365–3370.
 45. Filleul, S., et al. (2003). siRNA-mediated inhibition of vascular endothelial growth factor severely limits tumor resistance to antiangiogenic thrombospondin-1 and slows tumor vascularization and growth. *Cancer Res.* **63**: 3919–3922.
 46. Khalil, I. A., et al. (2004). Mechanism of improved gene transfer by the N-terminal stearylarginine: enhanced cellular association by hydrophobic core formation. *Gene Ther.* **11**: 636–644.
 47. Blessing, T., Remy, J. S., and Behr, J. P. (1998). Monomolecular collapse of plasmid DNA into stable virus-like particles. *Proc. Natl. Acad. Sci. USA* **95**: 1427–1431.
 48. Claffey, D. J., et al. (2000). Long chain arginine esters: a new class of cationic detergents for preparation of hydrophobic ion-paired complexes. *Biochem. Cell Biol.* **78**: 59–65.
 49. Lee, M., Nah, J.-W., Kwon, Y., Koh, J. J., Ko, K. S., and Kim, S. W. (2001). Water-soluble and low molecular weight chitosan-based plasmid DNA delivery. *Pharm. Res.* **18**: 427–431.